Running Title:

Determining the Relative Amounts of Positional Isomers in Complex Mixtures of Triglycerides Using Reverse-Phase HPLC-MS-MS

Michael Malone and Jason J. Evans*

University of Massachusetts Boston

Boston, MA 02125

Keywords;

triglycerides, triacylglycerols, HPLC, reverse-phase, mass spectrometry, MS-MS, CID, positional isomers

Address:

University of Massachusetts Boston

Chemistry Department

100 Morrissey Blvd.

Boston, MA 02125

* **University of Massachusetts Boston**

Chemistry Department

100 Morrissey Blvd.

Boston, MA 02125

Abbreviations: A, C:20:0, eicosanic acid; A_1, C20:1 (cis-11), eicosenoic acid; A_2, C20:2 (cis, cis-11, 14), eicosadienoic acid; amu., atomic mass units; APCI, atmospheric pressure chemical ionization; B, C22:0, behenic acid; CID, collision-induced decomposition; DAG, diglycerol; ESI, electrospray ionization; GC-MS, gas chromatography-mass spectrometry; L, C18:2 (cis, cis-9,12), linoleic acid; Lg, C24:0, Lignoceric acid; Ln, C18:3 (cis, cis, cis- 9,12,15), Linolenic acid; m/z, mass-to-charge ratio; MW, molecular weight; NICI, negative ion chemical ionization; O, (cis-9), oleic acid; P, C16:0, palmitic acid; P_1, C16:1 (cis-9), palmitoleic acid; RP-HPLC-MS-MS, reverse-phase high performance liquid chromatography tandem mass spectrometry; S, C18:0, stearic acid; TAGs, triglycerides.

Abstract

A reverse-phase high performance liquid chromatography-tandem mass spectrometry (RP-HPLC-MS-MS) method has been refined for the positional analysis of complex mixtures of triglycerides (TAGs). This method has the advantages of speed, ease of automation, and specificity over traditional digestion-based methods for the positional analysis of TAGs. Collisional-induced decomposition (CID) of ammoniated TAGs in an ion trap mass spectrometer produces spectra that are dependant on fatty acid position. Dominant diglycerol (DAG) fragments are formed from the loss of a fatty acid moiety from the ammoniated TAG species. Loss of fatty acids in the outer positions is favored over the loss of fatty acids in the central position. The combination of RP-HPLC and CID produce spectra that are free of isotope effects that can complicate spectral interpretation in existing methods. The combination also provides selectivity based on the chromatographic fractionation of TAGs, in addition, to the selectivity inherent in the CID process. Proof-of-concept experiments were performed with binary mixtures of TAGs from the SOS/SSO, OSO/OOS, and the PSO/POS/SPO positional isomer systems. Plots of fractional DAG fragment intensities vs. fractional composition of the binary mixtures are linear. These plots were used to determine the fractional composition of each of these isomeric systems in a variety of vegetable oils and animal fats. Current limitations, future developments, and applications of this method are discussed.

Introduction

Triglycerides (TAGs) consist of three fatty acid moieties attached to a glycerol backbone. The main biological function of TAGs is to serve as an energy source. Dietary TAGs are digested, reconstituted, and packaged as chylomicrons prior to entering the blood stream. Ultimately, the TAGs are delivered to cells in need of energy or stored as reserves in adipose tissue. Evidence is mounting that suggests TAG absorption [1-5], metabolism [1, 6-12], and atherogenic potential [2, 3, 13-23] (tendency for deposition of lipoproteins on the artery walls) may be influenced by fatty acid position. Additional work is needed in these areas to obtain a more complete understanding of the relationship between dietary lipids and heart disease. Development of efficient methods for the positional analysis of individual TAG species will facilitate the advance of these studies.

Positional analysis of TAGs has traditionally been performed through digestion of the outer two fatty acids and subsequent HPLC analysis of the resulting 2-monoglycerides and free fatty acids [2, 8, 24-27]. Commonly, complex mixtures of TAGs are digested in a single step and the overall fatty acid composition is compared to the position-specific fatty acid composition. These data have revealed general patterns, such that mono-unsaturated fatty acids are overwhelmingly favored in the center position and saturated fatty acids are favored in the outer positions for most animal and vegetable oils, suggesting that fatty acids are selectively attached to the glycerol backbone. Extensive work on the details of TAG biosynthesis [28-33] has explained the positional dependence of fatty acid composition. These studies have established that unique enzymes catalyze the

attachment of fatty acids onto each of the positions, and that these enzymes possess different fatty acid selectivities [34-42].

The digestion-based methods of positional analysis discussed above have been plagued with problems associated with fatty acid migration during digestion [43, 44]. In addition, these methods are cumbersome and time-consuming for investigations focusing on individual TAG species, since the mixtures must be fractionated prior to hydrolysis. Furthermore, the analysis of the hydrolysis products of co-eluting TAG species often produces ambiguous results.

Mass spectrometric methods have recently been developed that are less labor intensive, more conducive to performing positional analyses on individual TAG species, and more easily automated. Evershed and coworkers have used high performance liquid chromatography atmospheric pressure chemical ionization mass spectrometry (HPLC-APCI-MS) for this purpose [45-47]. The protonated TAGs formed during the APCI process acquire sufficient energy to fragment in the source. The major ions formed in the APCI process are the diglycerol (DAG) fragments, in which one of the fatty acid groups leaves the protonated TAG as a neutral fatty acid. Evershed's data show that fragmentation is less likely to occur at the center position than at the outer positions. The authors were able to predict which positional isomer was most abundant based on the DAG fragment of lowest relative abundance. The drawback of the APCI method is that many co-eluting TAGs produce common DAG fragments. As a result, it is often difficult to assign peaks to specific TAGs. In addition, it is not possible to de-convolute peak intensities, which would be necessary for quantification of positional isomers. These difficulties are

overcome to a great extent by combining RP-HPLC with the use tandem mass spectrometry (MS-MS).

Kallio and coworkers have used ammonia negative ion chemical ionization in conjunction with tandem mass spectrometry (NICI-MS-MS) for their analysis [48, 49]. The TAG sample is directly inserted into an ammonia CI source of a triple-quadrupole mass spectrometer via a probe and all of the TAGs are ionized under negative ion ammonia CI conditions, simultaneously. De-protonated TAGs are formed in the source and mass selected by the first quadrupole. These ions are transmitted to the second quadrupole for collision-induced dissociation (CID). The product ions are analyzed by a third quadrupole to produce a mass spectrum of the CID products. The most abundant fragment ions are deprotonated fatty acid fragments, but DAG-containing fragments (the information rich fragments) are fairly abundant peaks. CID affords a high level of selectivity, since ions of a particular mass-to-charge ratio are selected by the mass analyzer and subjected to CID. As a result, the analysis can be targeted to TAGs of a particular molecular weight. Direct analysis by tandem mass spectrometry without any chromatography to fractionate the TAGs can provide a wealth of information in a relatively short period of time (15-20 min.), even for very complex extracts. In this time frame a series of CID mass spectra can be acquired on several $[M-H]^-$ peaks of interest. However, this method has two main limitations. First of all, ^{13}C isotope contributions from TAGs that are lower in molecular weight by two mass units must be meticulously subtracted from the measured intensities, limiting the precision of the method. The DAG ions of interest in the CID spectra are often overwhelmed by other ^{13}C isotope-containing DAG fragments. Secondly, TAGs with the same molecular weight and one of the three

fatty acids in common, such as OOS and POA_1 will yield common DAG CID fragments, interfering with positional analysis. Nevertheless, Kallio was able to construct plots for some positional isomers that correlated the relative abundances of the DAG ions with the fractional composition. By contrast, the use of RP-HPLC prior to CID analysis completely eliminates the problems associated with ^{13}C isotope peaks because TAGs that differ by two mass units are generally completely separated chromatographically. The second limitation is also avoided in many cases by adequate separation of the interfering species. Data highlighting these advantages are presented in this work.

The analysis of TAGs by electrospray (ESI) mass spectrometry was first reported by Duffin and Henion [50]. They showed that the addition of ammonium acetate to the TAG sample could produce intense $[M+NH_4]^+$ ions, that are efficiently dissociated in CID experiments to form dominant DAG fragments indicative of the loss of the fatty acid moieties. Using an ESI-double focusing sector instrument, Cheng and Pittenauer observed that CID spectra of $[M+NH_4]^+$ from positional isomers were indistinguishable (PPO and POP produced the same CID spectra) [51]. Han and Gross obtained similar results with a triple-quadrupole instrument analyzing at the CID products of lithium adducts [52]. However, in an HPLC-ESI-MS-MS study with a triple-quadrupole instrument, Hvattum observed that the relative abundances of DAG fragments from ammoniated TAGs are dependant on fatty acid position [53], similar to Kallio's NICI experiments. Our experiments using an ion trap mass spectrometer also show that the CID spectra ammoniated TAGs are dependant on fatty acid position.

We report the use of RP-HPLC-ESI-MS-MS for fractional composition analysis of TAG positional isomers. This method combines the advantages of efficient

fractionation of the TAGs via RP-HPLC and enhanced selectivity provided by the CID process (DAG fragments derive from TAGs of only the selected molecular weight). This added degree of selectivity enables the quantification of many systems of positional isomers that would otherwise be difficult. The relative intensities of the DAG fragments in the CID spectrum of mixtures of positional isomers can be used to measure their relative abundances. Standard mixtures of positional isomers were analyzed and calibration plots of fractional DAG fragment intensities vs. fractional composition of three sets of positional isomers were constructed and used to determine the fraction composition of positional isomers in various vegetable oils and animal fats.

Experimental Procedures

The TAG designations that will be used throughout this paper consist of three letters, each indicating the presence of a particular fatty acid. The middle letter designates which fatty acid is in the center position. No distinction is made between the outer two positions. The standard symbols and one letter abbreviations used throughout the paper are listed as a footnote in the beginning of the paper.

HPLC grade methanol, n-propanol, n-butanol, methyl t-butyl ether (MTBE) were purchased from Acros (NJ). Ammonium formate (99%) was also purchased from Acros. Purified TAGs (LnLnLn, LLL, OOO, PPO, POP, SOS, SSO, POS, PSO, SPO, SSO, SOS, APO, POA, and PAO) were purchased from Larodan (Malmo, Sweeden). The unsaturated fatty acids contained in purchased TAGs were all in the *cis* configuration. The current study did not investigate possible differences in the relative intensities of diglycerol fragments between TAGs containing *cis* vs. *trans* fatty acids. Various

vegetable oils were purchased at the local supermarket. Fats from pork, chicken, and beef were carved from meat products purchased at the local supermarket.

Standards solutions of each of the pure TAGs were prepared in n-propanol at concentrations of 100±2 μM. Diluted standards (10.00 μM) for each were prepared in methanol/ammonium formate. These diluted standards were used to prepare standard solutions for a variety of different experiments that were performed in this work.

Extracts from various vegetable oils were prepared in 20 ml vials by dissolving a drop of oil in 15 ml n-PrOH. The extract was subsequently diluted 1:100 with methanol. A mixed extract was also prepared in this manner from a one drop each of peanut oil and corn oil. The fats were extracted into MTBE at 120 °C for one hour using the 20 ml vials and a variable temperature heating manifold. A drop of the extract was dissolved in 15 ml n-butanol and thoroughly dissolved. The resulting solution was diluted 1:100 in methanol in preparation for analysis.

Mass Spectrometer Parameters

A Thermofinnigan LCQ Advantage ion trap mass spectrometer (Sunnyvale, CA) was used to detect and characterize the TAGs. The connection from the syringe pump (direct injection experiments) or the HPLC column to the ESI source was made through a 1/16″ stainless steel zero-dead volume union and a 30 cm long, 50 μm ID, 185 μm OD, segment of fused silica capillary. The end of the fused silica capillary was fed into the ESI interface through a metal sheath. The tip of the capillary was carefully cut to provide a uniformly shaped tip. The tip of the capillary was positioned so that it was at the edge of the metal sheath. The electrospray cone is formed by applying a potential difference between the metal sheath and the ion transfer tube that focuses the ions into the mass

analyzer. The operating parameters of the ion trap mass spectrometer were as follows; capillary temperature (280 °C), spray voltage (4.00 kV), sheath gas (30 cm^3/min). CID was performed at a relative collision energy of 28 (unitless quantity) unless otherwise stated. This value should be applicable to other LCQ systems, assuming that the instrumental calibration procedures described by the manufacturer are carefully followed.

HPLC Parameters

A low-flow Shimadzu (Kyoto, Japan) HPLC system, which included a SCL-10A vp controller, two LC-10AD vp pumps, a SIL-10AD vp auto injector, and a 10 cm, 1 mm ID, 3 μm particle size, C_{18} BetaBasic column from ThermoElectron Corporation (Sunnyvale, CA) was used to separate the TAGs. The HPLC was operated at a flow rate of 35 μl/min (low flow pumps/no splitting necessary). A gradient elution was utilized, consisting of mobile phase A {methanol/n-propanol (80:20, by vol), saturated ammonium formate (≈ 1 mM), pH 7} and mobile phase B {methanol/n-propanol (20:80, by vol), saturated ammonium formate, pH 7. The Binary Gradient was as follows; 0 min/0 % A, 4 min/10 %, 36 min/60 % A, 38-40 min/85 % A. Injection volume was 5 μl for all samples (0.5-5.0 pmol of TAG on-column).

CID spectra of the Standards by direct infusion

The 10 μM diluted standards were each analyzed by direct infusion ESI-MS-MS (no HPLC column) using a syringe pump with a 500 μl syringe. The flow rate was 5 μl/min. The CID spectra were acquired under the conditions described above.

Analysis of a standard mixture and an oil extract by RP-HPLC-ESI-MS-MS

A mixture containing each of the standard TAGs at concentrations of about 0.7 μM was prepared in methanol using the diluted standards described above. This mixture

was analyzed by RP-HPLC-MS in the MS-only mode and in a targeted RP-HPLC-MS-MS mode. In the MS-only mode a mass spectrum of the ions formed in the electrospray process was produced at a rate of about 1 spectrum per second throughout the course of the chromatographic run. The targeted MS-MS analysis was developed based on the retention times determined from the experiment performed in the MS-only mode. In this targeted mode the mass spectrometer was programmed to select the appropriate m/z ratio for CID analysis during a 2-3 minute chromatographic time window corresponding to the eluting TAG. The mixed extract of peanut/corn oil was also analyzed in the MS-only targeted MS-MS modes.

Experiments performed to construct calibration plots

The 10 μM standards SOS, SSO, OSO, OOS, PSO, SPO, and POS were used to prepare known binary mixtures of positional isomers. Standard mixtures of the following pairs of positional isomers were prepared; SOS/SSO, OSO/OOS, POS/SPO, PSO/POS, and SPO/PSO. The sum of the concentrations for the pair of positional isomers for each of the standard mixtures was 1 μM. The fractions of a positional isomer in the binary mixtures ranged from 0.00-1.00 in increments of 0.10. Each of the standard mixtures was analyzed by a targeted RP-HPLC-MS-MS method designed specifically for these three systems of positional isomers. The oil and fat extracts described above were also analyzed by this method in efforts to perform a positional analysis of various oils and fats for these three systems of positional isomers.

Data Analysis

The spectra used in this work to define the intensities of the DAG fragments are the composite average of 50 spectra, unless otherwise stated. Regression parameters for

the calibration plots were used to calculate the fractional composition of various vegetable based oils and animal fats. For the SSO/SOS and OOS/OSO systems the linear regression data from the calibration plots were used directly. Repeated measurements of samples over the course of several months suggest that this method measures the ratio of DAG fragment ions are reproducible to within ± 5 %. The average relative standard error of the OOS/OSO and SSO/SOS calibration plots was 0.005 and 0.007, respectively, giving relative errors in the predicted fractions of ≈ 2-5 % (≈ standard error/slope). For the POS/SPO/PSO system, the linear regression data from the three calibration plots were used to construct three simultaneous equations that were used to solve for the fractional composition data for each of the three positional isomers in the each of the samples. The errors in the fractions were found through the application of a Monte Carlo analysis. Our Monte Carlo approach uses repeated iterations (N=10000) of solving the simultaneous equations, while randomly modulating the error in the input ion ratios obtained from the analysis of the oil and fat samples within a 5 % tolerance. The results give Gaussian distributions for each of the fractions. The standard deviations of these distributions are reported as reasonable estimates of the errors. This Monte Carlo analysis was performed using Mathematica 4.2.

Results

Direct infusion CID spectra of each of the standard TAGs

The CID spectrum for each of the standard TAGs was acquired via direct infusion ESI-MS-MS. Figure 1 shows the CID spectrum of POS. This spectrum is zoomed in on the DAG fragments ($[M + NH_4 - FA+NH_3]^+$), which are the most intense fragment ions under these experimental conditions. These ions are presumably formed via the loss of a

neutral fatty acid and ammonia. The fragment ions resulting from the loss of the oleate moiety are of significantly lower abundance than the fragment ions resulting from loss of the palmitate and stearate moieties. It is speculated that fragmentation initiates at the ammoniated fatty acid group and that adduct formation at the center fatty acid position is less probable, perhaps as consequence of steric hindrance. The relative intensities of diglyceride fragments in the CID spectra of all of the TAG standards studied in this work are listed in Table 1. The less favorable loss of the fatty acid from the center position appears to be universal for all TAGs. Other trends that can be observed from careful inspection of Table 1 is that fragmentation at a particular position increases with increasing degree of unsaturation, and, though to a lesser extent, with increasing chain length. Assuming that the mechanism for fragmentation given above is correct (fragmentation occurs at the ammoniated fatty acid), these trends can be rationalized on the basis of ammonium ion affinities, which are likely to increase with increasing degree of unsaturation and fatty acid chain length[54].

Chromatography

Figure 2a shows a chromatogram for the standard mixture of TAGs. Figure 2b shows a chromatogram of the peanut oil/corn oil extract. The data was collected in MS only mode. Our data show that retention increases for TAGs with FAs of longer chain lengths and lower degrees of unsaturation. These observations agree with previously reported data illustrating that retention of TAGs species in RP-HPLC can be predicted reasonably well based on the sum of empirically-derived retention factors for the constituent fatty acid groups.[55] The major TAG species present in the standard mixture are labeled on the chromatogram shown in Figure 2a.

In addition, targeted CID experiments were performed on the standard mixture and the peanut oil/corn oil extract. For the standard mixture the CID spectra of the m/z 878 and m/z 904 peaks, which correspond to the positional isomer systems of POS/PSO/SPO and SOO/OSO, respectively, were examined to investigate the extent at which positional isomers co-elute. In both cases it was found the ratios of the relative intensities of the DAG fragments do not vary as one moves across a chromatographic peak. This indicates little to no fractionation of positional isomers of TAGs occurs in our reverse-phase HPLC method.

The masses and relative intensities of the DAG fragments from the targeted MS-MS experiments were used to identify the major and minor TAG species in the peanut oil/corn oil extract. Labels indicating these identified species have noted above the chromatographic peaks in Figure 2b. Each labeled species is the most abundant positional isomer of its system. The dominance of the unsaturated fatty acids in the center position is apparent. Figure 3a is also data from the targeted CID experiment on the peanut/corn oil extract. It shows the total ion chromatogram of the CID products of TAGs that have a MW of 884.5 amu ($[M+NH_4]^+$ ion at m/z 902.6). The chromatogram indicates that TAGs of the same molecular weight have been partially fractionated by the RP-HPLC method. Figure 3b shows the average CID spectrum across these fractionated chromatographic peaks. The intense peak at m/z 603.3 corresponds to OO^+ or LS^+, and the peaks at m/z 601.3 and m/z 605.4 correspond to LO^+ and SO^+, respectively. These DAG fragments indicate the dominant presence of OOO and LOS/LSO/SLO in the oil mixture.

Advantages of using HPLC in conjunction with CID analysis

To highlight the advantages of combining HPLC and CID, experiments were designed to directly compare RP-HPLC-MS-MS data with direct infusion-MS-MS data. The sample used for this comparison was the peanut oil/corn oil mixture. Figure 4a is the CID of the m/z 900.5 peak acquired under direct infusion analysis. Figure 4b is the CID spectrum of the m/z 900.5 peak (TAGs of MW 882.5 amu) acquired during a targeted RP-HPLC-MS-MS analysis. The key DAG peaks in these spectra consist of m/z 599.3 (LL^+), m/z 601.3 (OL^+), and m/z 603.3 (OO^+ and LS^+), indicating the presence of the OOL/OLO and SLL/LSL systems at m/z 900.5. The intensities of the peaks in the targeted MS-MS data suggest that OOL and SLL are the dominant positional isomers. In comparison, the direct infusion analysis is difficult to interpret because DAG fragments from the corresponding ^{13}C isotope peaks of ammoniated TAGs of MW 880.5 amu have a dominant presence in the spectrum, as evident from the peaks at m/z 600 and 602. TAG species that contain two ^{13}C's can produce DAG fragments containing two, one, or no ^{13}C isotopes, and as a result, some of intensity at the m/z 599, 601, and 603 peaks also result from these ^{13}C-containing fragment ions. Another factor contributing to the complexity of the spectra results from the limited trapping resolution of the ion trap. It is possible that some ^{13}C containing ions at m/z 899.5 may also be trapped and fragmented. These complications are not present in the HPLC-MS-MS analyses. The TAGs that produce ammoniated ions at m/z 898 and 900 are completely separated, thus, removing these isotope effects. In addition, it is also clearly evident through a direct comparison of the two spectra that the ratios among the m/z 599.3, m/z 601.3, and m/z 603.3 ions are altered by these isotope effects. As a result, quantification of positional isomers using the direct infusion method would yield erroneous results.

Partial fractionation of isomeric TAGs species by HPLC-MS-MS in some cases can be useful in the quantification of positional isomers. As mentioned previously, it is evident from Figure 3 that our RP-HPLC analysis partially resolved TAGs that form $[M+NH_4^+]$ ions at m/z 902.6. The CID spectrum obtained from averaging 18 scans from 18.0 to 18.5 minutes is shown in Figure 5a, and the CID spectrum of the latter eluting TAGs are shown in Figure 5b, which was obtained by carefully subtracting the contribution from the earlier eluting peak. Analysis of Figure 5a shows only one diglycerol peak at m/z 603.3. This ion corresponds to OO^+, confirming the identity of the earlier eluting TAG as OOO. Analysis of Figure 5b shows DAG peaks at m/z 601.3, 603.3, and 605.3, as well as, ions of lower intensity at m/z 575.3 and 629.4. These ions correspond to OL^+, SL^+, OS^+/PA_1^+, PL^+, and A_1L^+, respectively, confirming the identities of latter eluting TAGs as LOS/LSO/SLO and $A_1LP/LA_1P/A_1PL$ positional isomers. The intensities of these DAG peaks suggest that LOS is likely to be the dominant positional isomer of the LOS/LSO/SLO in these oils. The minor presence of $A_1LP/LA_1P/A_1PL$ positional isomers would not interfere to any great extent with the relative quantification of the LOS/LSO/SLO system. Figure 5c illustrates the average CID spectrum of the m/z 902.5 ion acquired via direct infusion-ESI-MS-MS. Interpretation of this spectrum is difficult, as discussed above. Quantitative analysis of the LOS/LSO/SLO system is not possible from this spectrum. Furthermore, the diglycerol peaks indicating the presence of the $A_1LP/LA_1P/A_1PL$ positional isomers are lost in the background noise. The enhanced S/N ratio is, yet, another advantage of combining HPLC and CID analysis.

Quantification of positional isomers

The CID spectrum of $[M+NH_4]^+$ for a given mixture of positional isomers corresponds to a weighted average of each the positional isomers in the mixture. Since positional isomers co-elute, as highlighted above, the CID spectra from targeted RP-HPLC-MS-MS analyses contain fractional composition information. To obtain this fractional composition information calibration curves are useful. To illustrate the utility of such calibration plots, binary mixtures of the SOP/SPO/PSO, OSO/OOS, and SOS/SSO positional isomer systems were analyzed by targeted RP-HPLC-MS-MS. Figure 6 presents these calibration plots for the five sets of binary mixtures analyzed in these experiments. The fractional peak intensities of the DAG fragments are plotted against the mole fraction of the positional isomers. A linear relationship is apparent from the data.

These calibration plots were applied to the positional analysis of these systems of positional isomers in several vegetable oils and animal fats. Table 2 shows results from these experiments. The results agree with previous data from the traditional digestion methods [7, 8, 56, 57] and mass spectrometric data [45, 46, 49]. For the vegetable based oils and beef and chicken fat, the oleate moiety is placed in the center position of the TAGs almost exclusively for the systems examined in this study. In contrast, but consistent with the results of others, the palmitate moiety is favored at the center position for the POS/SPO/PSO system in pork fat (essentially 100 % of this positional isomer is in the SPO form). Also, the stearate moiety is favored in the center position (90 %) for the SSO/SOS system in pork fat.

The errors associated with the POS/PSO/SPO system are greater than the errors associated with the SSO/SOS and OSO/OOS systems due to a propagation of the errors

of the regression parameters from the three calibration plots. This propagation is inherent in the Monte Carlo simulations. Nevertheless, fractional compositions for the POS/SPO/PSO systems were determined to within ± 0.1.

Determining reliable fractional composition data for a given system, such as the POS/SPO/PSO, SSO/SOS, and OSO/OOS systems examined in this study, can be complicated by the presence of other isomeric species with different fatty acid compositions that happen to co-elute. For example, with the analysis of the SSO/SOS system in peanut oil, the CID of the m/z 906.5 ion (the mass of the ammoniated parent from SSO/SOS) produces intense DAG fragments at m/z 577 and m/z 631, corresponding to PO^+ and AO^+, respectively. This indicates a significant presence of the co-eluting POA/OPA/PAO TAG system in peanut oil. The loss of the oleate moiety from these TAGs produces a peak at m/z 607 (PA^+), as does the loss of oleate from SSO and SOS (SS^+). One can not differentiate the portion of the m/z 607 peak that is attributable to the SOS/SSO system from the portion attributable to the POA/OPA/PAO TAG system, and, as a result, fractional composition data is unattainable. Due to abundant presence of the POA/OPA/PAO TAGs, reliable data for the SSO/SOS system could not be obtained for many of the oils. The $A_1PO/A_1OP/OA_1P$ system of positional isomers co-elutes with the OSO/OOS system, and, therefore can interfere with its quantitative positional analysis. The $A_1PO/A_1OP/OA_1P$ TAGs were only very minor components in the oils that we investigated and did not greatly effect quantification of the SOS/SSO system. However, the $A_1PO/A_1OP/OA_1P$ TAGs were present in significant amounts in pig fat, making reliable data for the OSO/OOS system unattainable. Further research is in progress that will attempt to address the limitations that some co-eluting isomeric TAG species place

on the current methodology. The direction of this future research is briefly described in the discussion section of this paper.

Discussion

This paper illustrates that calibration plots for systems of positional isomers can be constructed and used to measure the fractional compositions of positional isomers in complex mixtures. Further work will be performed to extend this work to other isomeric systems, including the development of a model that can predict the relative intensities of the DAG fragments in the CID spectrum of any ammoniated TAG. Additional investigations will also focus evaluating the chromatographic and CID characteristics of TAGs containing *cis* vs. *trans* fatty acids.

The method described in this paper has the advantages of providing CID spectra that are easier to interpret and give more precise quantitative information. The spectra are easier to interpret as a result of the elimination of ^{13}C isotope effects. The added precision results from both the removal of the ^{13}C isotope effects, as well as, the added selectivity obtained by combining HPLC with CID. Only co-eluting TAGs of the same molecular weight that yield a common CID product interfere with quantitative positional analysis. Thus, the possible interferences have been significantly reduced. However, interferences do still occur when analyzing certain TAG species, and overcoming these difficulties is a challenge that lies ahead.

Improvements in the chromatographic resolution of the TAGs may help to separate some of the interfering species. The RP-HPLC method used in this work was optimized for the methanol/n-propanol (ammonium formate) mobile phase system. However, better separations have been reported in the literature and it may be possible to

improve on our current HPLC method [55, 58, 59]. Future work will include an investigation of different mobile phase systems that may be compatible with the formation of $[M+NH_4]^+$ ions..

$(MS)^3$ experiments have proven to be very powerful for some applications, and may be a useful approach for dealing with these interferences. In this approach, DAG fragments of a certain m/z ratio formed in the first CID event are isolated in the ion trap and subjected to another round of CID. The following example for the SOS/SSO system is offered as an illustration of the potential application of $(MS)^3$ experiments. As mentioned above, the DAG peak at m/z 607 can be formed via CID of the TAGs from both the SOS/SSO (SS^+) and PAO/APO/AOP (AP^+) systems. Once formed, if these fragments are isolated in the ion trap and subsequently dissociated in another round of CID, monoglycerol fragments may be produced corresponding to the free fatty acid fragments, S, O, A, and P. The ratio of intensities for the O and S monoglyceride products would likely be indicative of the fractional composition of the SOS/SSO, and the relative abundances of the intensities for the A and P monoglyceride products would likely be indicative of the fractional composition of the PAO/APO/AOP. These $(MS)^3$ experiments are currently under investigation. Initial work has proven to be challenging because the intensities of the monoglycerol fragments are very low. However, we are attempting to fine-tune the conditions necessary to produce useful $(MS)^3$ data.

Upon further development we plan to utilize this method to investigate the influence of fatty acid position on metabolism, absorption, transport, biosynthesis, and mobilization of essentially any set of positional TAG isomers in biological systems. The

kinetics of these processes will be studied for systems of positional isomers using stable isotope incorporation in conjunction with this methodology.

Acknowledgment

The LC-MS used in this work was acquired through partial support from the NSF.

References

1. Kubow, S. The Influence of Positional Distribution of Fatty Acids in Native, Interestified, and Structure-Specific Lipids on Lipoprotein Metabolism and Atherogenesis. *Journal of Nutritional Biochemistry* **7**, 530-541 (1996).
2. Filer, L.J., Jr., Mattson, F.H. & Fomon, S.J. Triglyceride configuration and fat absorption by the human infant. *J Nutr* **99**, 293-298 (1969).
3. Lien, E.L., Boyle, F.G., Yuhas, R., Tomarelli, R.M. & Quinlan, P. The effect of triglyceride positional distribution on fatty acid absorption in rats. *J Pediatr Gastroenterol Nutr* **25**, 167-174 (1997).
4. Renaud, S.C., Ruf, J.C. & Petithory, D. The positional distribution of fatty acids in palm oil and lard influences their biologic effects in rats. *J Nutr* **125**, 229-237 (1995).
5. Summers, L.K. et al. Use of structured triacylglycerols containing predominantly stearic and oleic acids to probe early events in metabolic processing of dietary fat. *J Lipid Res* **40**, 1890-1898 (1999).
6. Decker, E.A. The role of Steriospecific Saturated Fatty Acid Positionss on Lipid Metabolism. *Nutr. Review* **54**, 108-110 (1996).
7. Brockerhoff, H., Hoyle, R.J. & Wolmark, N. Positional distribution of fatty acids in triglycerides of animal depot fats. *Biochim Biophys Acta* **116**, 67-72 (1966).
8. Brockerhoff, H. & Yurkowski, M. Stereospecific analyses of several vegetable fats. *J Lipid Res* **7**, 62-64 (1966).
9. Nawar, W.W. Lipids, Edn. 3rd. (Marcel Dekker, Inc., New York; 1996).
10. Small, D.M. The effects of glyceride structure on absorption and metabolism. *Annu Rev Nutr* **11**, 413-434 (1991).
11. Padley, F.B., Gunstone, F.D. & Harwood, J.L. Occurrence and Characteristics of Oils and Fats, Edn. 2nd. (Chapman & Hall, London; 1994).
12. Kritchevsky, D. Effects of triglyceride structure on lipid metabolism. *Nutr Rev* **46**, 177-181 (1988).
13. Hunter, J.E. Studies on effects of dietary fatty acids as related to their position on triglycerides. *Lipids* **36**, 655-668 (2001).
14. Kritchevsky, D., Tepper, S.A., Chen, S.C., Meijer, G.W. & Krauss, R.M. Cholesterol vehicle in experimental atherosclerosis. 23. Effects of specific synthetic triglycerides. *Lipids* **35**, 621-625 (2000).
15. Kritchevsky, D., Tepper, S.A., Kuksis, A., Wright, S. & Czarnecki, S.K. Cholesterol Vehicle in Experimental Atherosclerosis. 22. Refined, Bleached, Deodorized (RBD) Palm Oil, Randomized Palm Oil and Red Palm Oil. *Nutritional research* **20**, 887-892 (2000).
16. Summers, L.K., Fielding, B.A., Ilic, V., Quinlan, P.T. & Frayn, K.N. The effect of triacylglycerol-fatty acid positional distribution on postprandial metabolism in subcutaneous adipose tissue. *Br J Nutr* **79**, 141-147 (1998).
17. Kritchevsky, D., Tepper, S.A. & Klurfeld, D.M. Lectin may contribute to the atherogenicity of peanut oil. *Lipids* **33**, 821-823 (1998).
18. Kritchevsky, D., Tepper, S.A., Kuksis, A., Eghtedary, K. & Klurfeld, D.M. Cholesterol Vehicle in Experimental Atherosclerosis. 21. Native and Randomized Lard and Tallow. *Journal of Nutritional Biochemistry* **9**, 582-585 (1998).

19. Kritchevsky, D., Tepper, S.A., Wright, S., Kuksis, A. & Hughes, T.A. Cholesterol Vehicle in Experimental Atherosclerosis. 20. Cottonseed Oil and Randomized Cottonseed Oil. *Nutritional Research* **18**, 259-264 (1998).
20. Aoyama, T. et al. Absorption and metabolism of lipids in rats depend on fatty acid isomeric position. *J Nutr* **126**, 225-231 (1996).
21. Pufal, D.A., Quinlan, P.T. & Salter, A.M. Effect of dietary triacylglycerol structure on lipoprotein metabolism: a comparison of the effects of dioleoylpalmitoylglycerol in which palmitate is esterified to the 2- or 1(3)-position of the glycerol. *Biochim Biophys Acta* **1258**, 41-48 (1995).
22. Lien, E.L., Yuhas, R.J., Boyle, F.G. & Tomarelli, R.M. Corandomization of fats improves absorption in rats. *J Nutr* **123**, 1859-1867 (1993).
23. Kritchevsky, D., Tepper, S.A., Vesselinovitch, D. & Wissler, R.W. Cholesterol vehicle in experimental atherosclerosis. 13. Randomized peanut oil. *Atherosclerosis* **17**, 225-243 (1973).
24. Brockerhoff, H. Stereospecific analysis of triglycerides: an alternative method. *J Lipid Res* **8**, 167-169 (1967).
25. Brockerhoff, H. & Ackman, R.G. Positional distribution of isomers of monoenoic fatty acids in animal glycerolipids. *J Lipid Res* **8**, 661-666 (1967).
26. Slakey, P.M. & Lands, W.E.M. The Structure of Rat Liver Triglycerides. *Lipids* **3**, 30-36 (1967).
27. Akesson, B. Composition of rat liver triacylglycerols and diacylglycerols. *Eur J Biochem* **9**, 463-477 (1969).
28. Brown, J.L. & Johnston, J.M. The Utilization of I- and 2-Monoglycerides for Intestinal Triglyceride Biosynthesis. *Biochim Biophys Acta* **84**, 448-457 (1964).
29. Pieringer, R.A., Bonner, H., Jr. & Kunnes, R.S. Biosynthesis of phosphatidic acid, lysophosphatidic acid, diglyceride, and triglyceride by fatty acyltransferase pathways in Escherichia coli. *J Biol Chem* **242**, 2719-2724 (1967).
30. Polheim, D., David, J.S., Schultz, F.M., Wylie, M.B. & Johnston, J.M. Regulation of triglyceride biosynthesis in adipose and intestinal tissue. *J Lipid Res* **14**, 415-421 (1973).
31. Lehner, R. & Kuksis, A. Biosynthesis of triacylglycerols. *Prog Lipid Res* **35**, 169-201 (1996).
32. Sorger, D. & Daum, G. Synthesis of triacylglycerols by the acyl-coenzyme A:diacyl-glycerol acyltransferase Dga1p in lipid particles of the yeast Saccharomyces cerevisiae. *J Bacteriol* **184**, 519-524 (2002).
33. Sorger, D. & Daum, G. Triacylglycerol biosynthesis in yeast. *Appl Microbiol Biotechnol* **61**, 289-299 (2003).
34. Brown, A.P., Slabas, A.R. & Denton, H. Substrate selectivity of plant and microbial lysophosphatidic acid acyltransferases. *Phytochemistry* **61**, 493-501 (2002).
35. Reeves, C.D. et al. Alteration of the substrate specificity of a modular polyketide synthase acyltransferase domain through site-specific mutations. *Biochemistry* **40**, 15464-15470 (2001).
36. Holub, B.J. The suitability of different acyl acceptors as substrates for the acyl-Coa : 2-acyl-sn-glycero-3-phosphorylcholine acyltransferase in rat liver microsomes. *Biochim Biophys Acta* **664**, 221-228 (1981).

37. Holub, B.J. & Piekarski, J. The relative utilization of different molecular species of unsaturated 1,2-diacyglycerols by the acyl-CoA:1,2-diacyl-sn-glycerol acyltransferase in rat liver microsomes. *Can J Biochem* **55**, 1186-1190 (1977).
38. Ichihara, K., Takahashi, T. & Fujii, S. Diacylglycerol acyltransferase in maturing safflower seeds: its influences on the fatty acid composition of triacylglycerol and on the rate of triacylglycerol synthesis. *Biochim Biophys Acta* **958**, 125-129 (1988).
39. Ichihara, K., Asahi, T. & Fujii, S. 1-Acyl-sn-glycerol-3-phosphate acyltransferase in maturing safflower seeds and its contribution to the non-random fatty acid distribution of triacylglycerol. *Eur J Biochem* **167**, 339-347 (1987).
40. Okuyama, H., Yamada, K., Ikezawa, H. & Wakil, S.J. Factors affecting the acyl selectivities of acyltransferases in Escherichia coli. *J Biol Chem* **251**, 2487-2492 (1976).
41. Okuyama, H., Yamada, K. & Ikezawa, H. Accepton concentration effect in the selectivity of acyl coenzyme A: U aclglycerylphosphorylcholine acyltransferase system in rat liver. *J Biol Chem* **250**, 1710-1713 (1975).
42. Yamada, K. & Okuyama, H. Selectivity of diacylglycerophosphate synthesis in subcellular fractions of rat liver. *Arch Biochem Biophys* **190**, 409-420 (1978).
43. Brockerhoff, H. A Stereospecific Analysis of Triglycerides. *J Lipid Res* **79**, 10-15 (1965).
44. Jensen, R.G., Sampugna, J., Carpenter, D.L. & Pitas, R.E. Structural analysis of triglyceride classes obtained from cow's milk fat by fractional crystallization. *J Dairy Sci* **50**, 231-234 (1967).
45. Mottram, H.R., Woodbury, S.E. & Evershed, R.P. Identification of Triacylgylcerol Potional Isomers Present in Vegetable Oils by High Performance Liquid Chromatography/Atmospheric Pressure Chemical Ionization Mass Spectrometry. *Rapid Commun Mass Spectrom* **11**, 1240-1252 (1997).
46. Mottram, H.R., Crossman, Z.M. & Evershed, R.P. Regiospecific characterisation of the triacylglycerols in animal fats using high performance liquid chromatography-atmospheric pressure chemical ionisation mass spectrometry. *Analyst* **126**, 1018-1024 (2001).
47. Mottram, H.R. & Evershed, R.P. Elucidation of the composition of bovine milk fat triacylglycerols using high-performance liquid chromatography-atmospheric pressure chemical ionisation mass spectrometry. *J Chromatogr A* **926**, 239-253 (2001).
48. Kallio, H., Yli-Jokipii, K., Kurvinen, J.P., Sjovall, O. & Tahvonen, R. Regioisomerism of triacylglycerols in lard, tallow, yolk, chicken skin, palm oil, palm olein, palm stearin, and a transesterified blend of palm stearin and coconut oil analyzed by tandem mass spectrometry. *J Agric Food Chem* **49**, 3363-3369 (2001).
49. Currie, G.J. & Kallio, H. Triacylglycerols of human milk: rapid analysis by ammonia negative ion tandem mass spectrometry. *Lipids* **28**, 217-222 (1993).
50. Duffin, K.L., Henion, J.D. & Shieh, J.J. Electrospray and tandem mass spectrometric characterization of acylglycerol mixtures that are dissolved in nonpolar solvents. *Anal Chem* **63**, 1781-1788 (1991).

51. Cheng, C., Gross, M.L. & Pittenauer, E. Complete structural elucidation of triacylglycerols by tandem sector mass spectrometry. *Anal Chem* **70**, 4417-4426 (1998).
52. Han, X. & Gross, R.W. Quantitative analysis and molecular species fingerprinting of triacylglyceride molecular species directly from lipid extracts of biological samples by electrospray ionization tandem mass spectrometry. *Anal Biochem* **295**, 88-100 (2001).
53. Hvattum, E. Analysis of triacylglycerols with non-aqueous reversed-phase liquid chromatography and positive ion electrospray tandem mass spectrometry. *Rapid Commun Mass Spectrom* **15**, 187-190 (2001).
54. Evans, J., Nicol, G. & Munson, B. Proton affinities of saturated aliphatic methyl esters. *J Am Soc Mass Spectrom* **11**, 789-796 (2000).
55. Sjovall, O., Kuksis, A., Marai, L. & Myher, J.J. Elution factors of synthetic oxotriacylglycerols as an aid in identification of peroxidized natural triacylglycerols by reverse-phase high-performance liquid chromatography with electrospray mass spectrometry. *Lipids* **32**, 1211-1218 (1997).
56. Christie, W.W. & Moore, J.H. A comparison of the structures of triglycerides from various pig tissues. *Biochim Biophys Acta* **210**, 46-56 (1970).
57. Christie, W.W. & Moore, J.H. The structure of egg yolk triglycerides. *Biochim Biophys Acta* **218**, 83-88 (1970).
58. Byrdwell, W.C., Neff, W.E. & List, G.R. Triacylglycerol analysis of potential margarine base stocks by high-performance liquid chromatography with atmospheric pressure chemical ionization mass spectrometry and flame ionization detection. *J Agric Food Chem* **49**, 446-457 (2001).
59. Jham, G.N., Nikolova-Damyavova, B., Viera, M., Natalino, R. & Rodrigues, A.C. Determination of the triacylglycerol composition of coffee beans by reverse-phase high-performance liquid chromatography. *Phytochem Anal* **14**, 310-314 (2003).

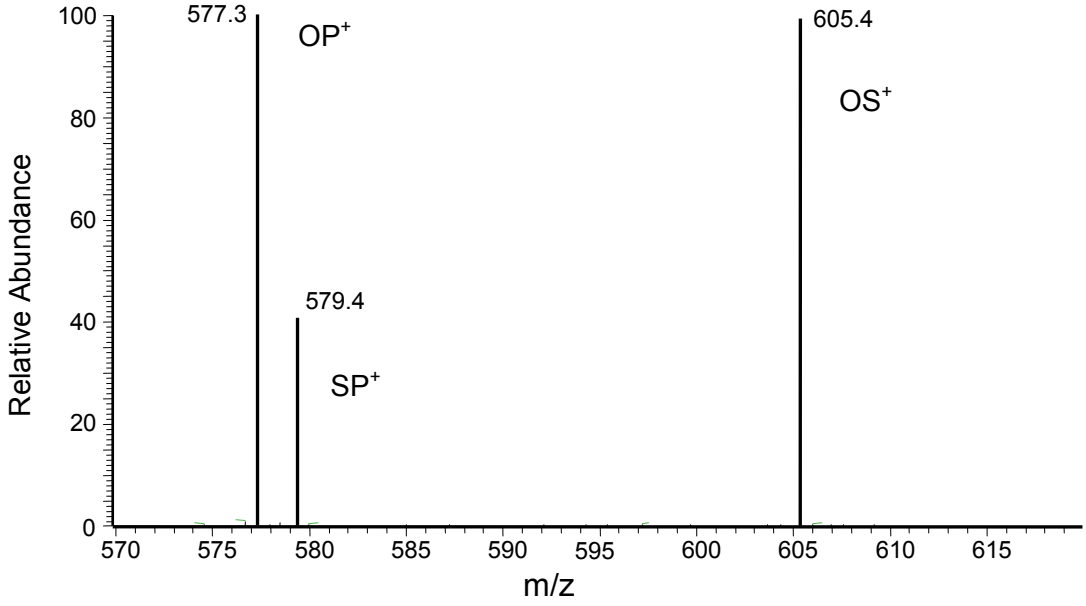

Figure 1. CID spectrum of POS. The SP^+ that forms from the loss of the oleate moiety from the center position is the diglycerol fragment of lowest abundance.

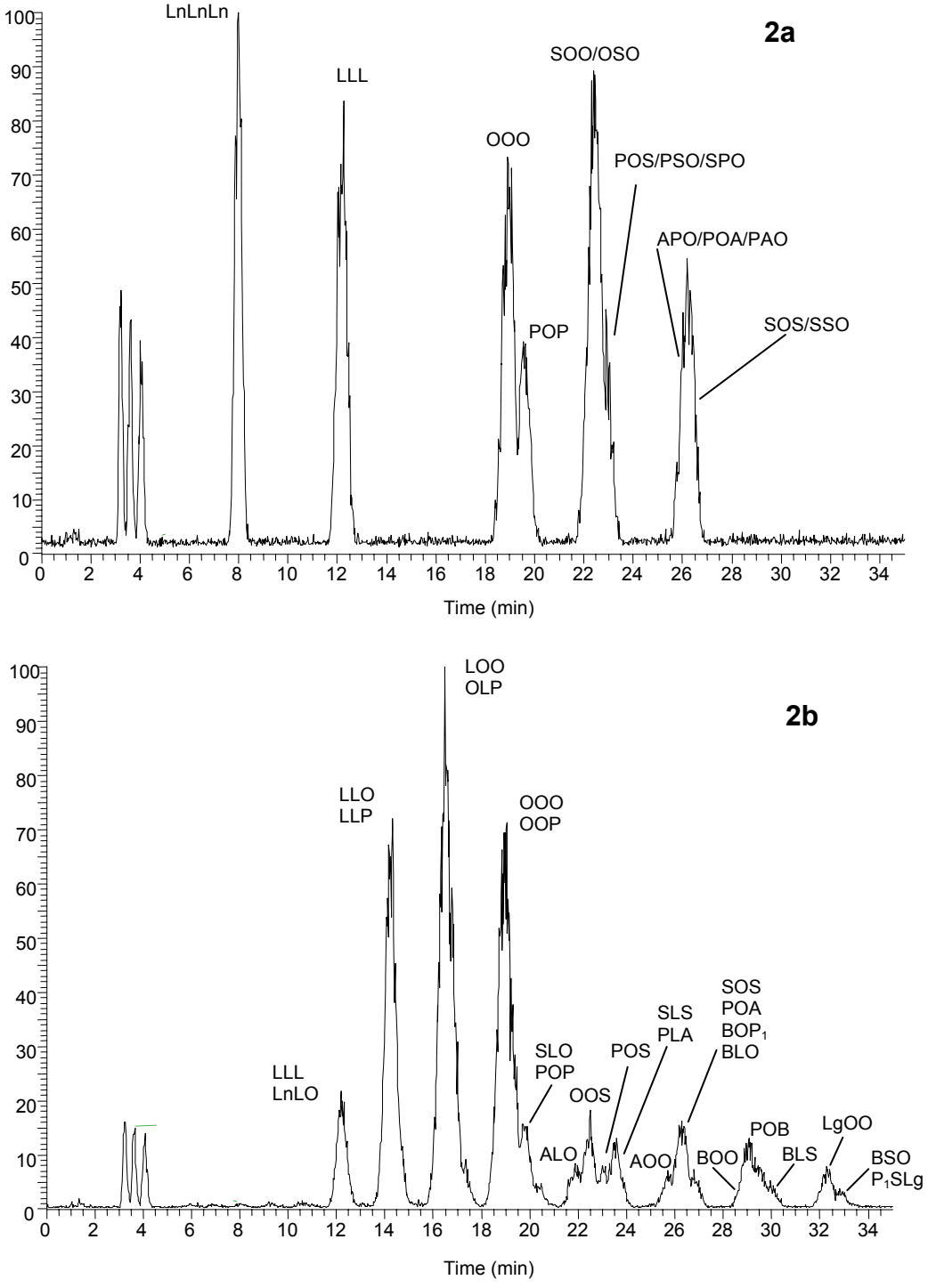

Figure 2. Ion chromatograms from m/z 800-1000 for the standard TAG mixture (2a) and an extract of a mixture of peanut and corn oils (2b). The masses and intensities of the diglycerol fragments in the CID spectra were used to identify the major TAG species.

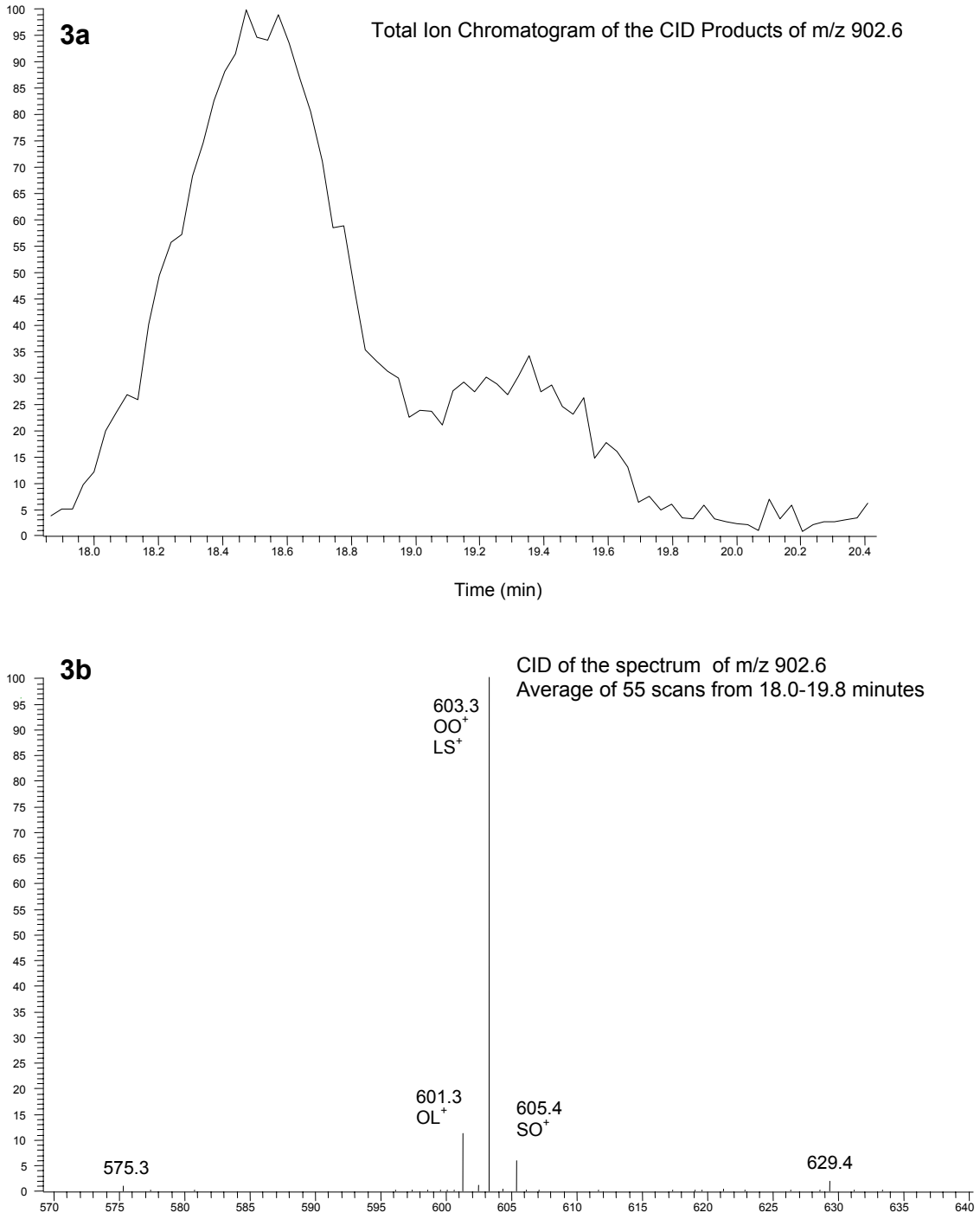

Figure 3. Above: The total ion chromatogram of the CID products of the m/z 902.6 ion from a targeted MS-MS analysis (3a). The chromatogram shows clear signs of TAGs that have been partially fractionated by the RP-HPLC method. Below: The average CID spectrum across the fractionated chromatographic peaks (3b). The masses of the diglycerol peaks suggest the presence of OOO and LOS/LSO/SLO.

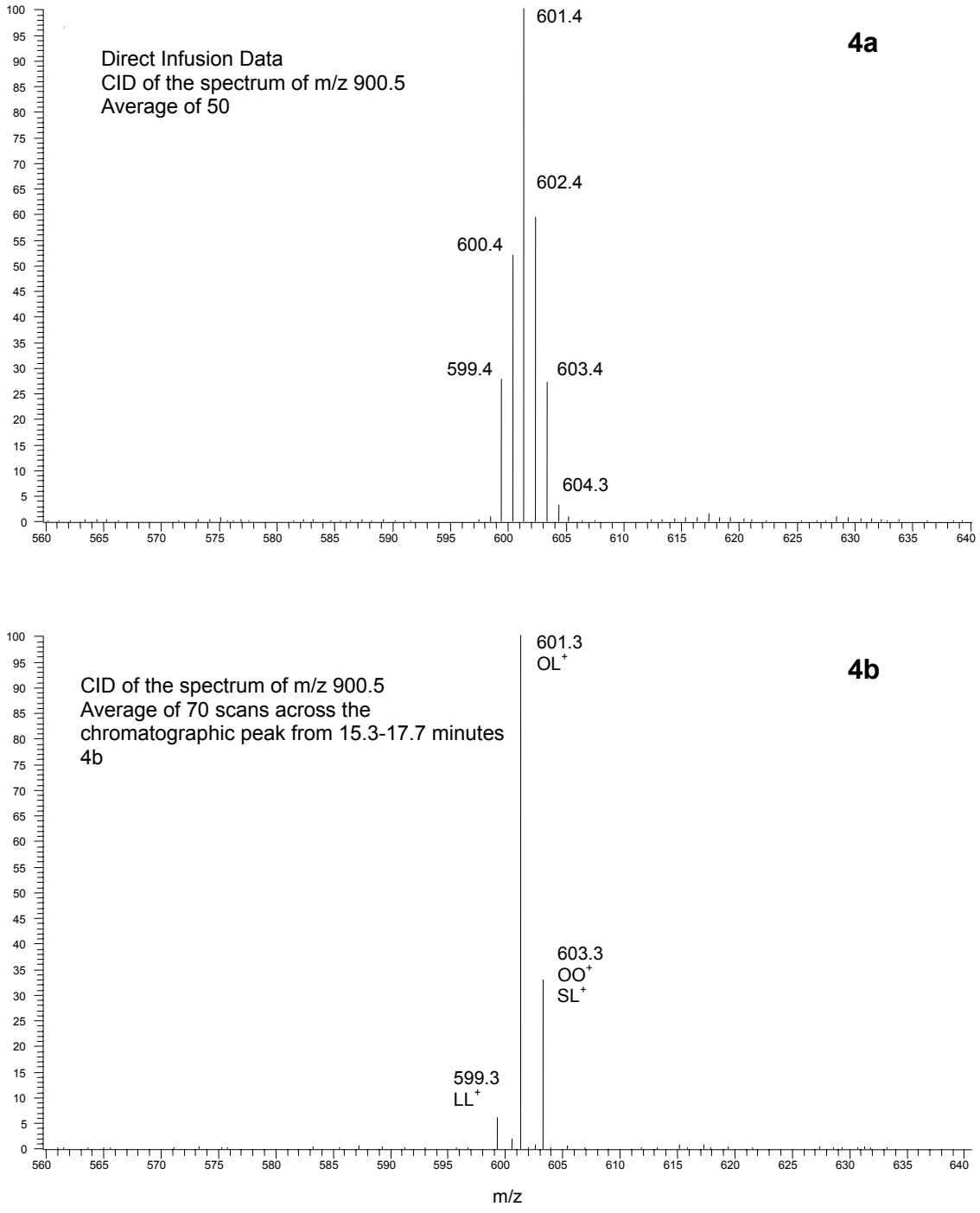

Figure 4. The above spectrum is the average CID spectrum of the m/z 900.6 ion acquired via direct infusion MS-MS of the peanut oil/corn oil mixture (4a). Shown below is the average CID spectrum of the m/z 900.6 ion acquired via RP-HPLC-MS-MS of the peanut oil/corn oil mixture (4b). The major advantage of using HPLC to fractionate the TAGs prior to CID analysis is the removal of interfering ^{13}C isotope effects present in the direct infusion spectra.

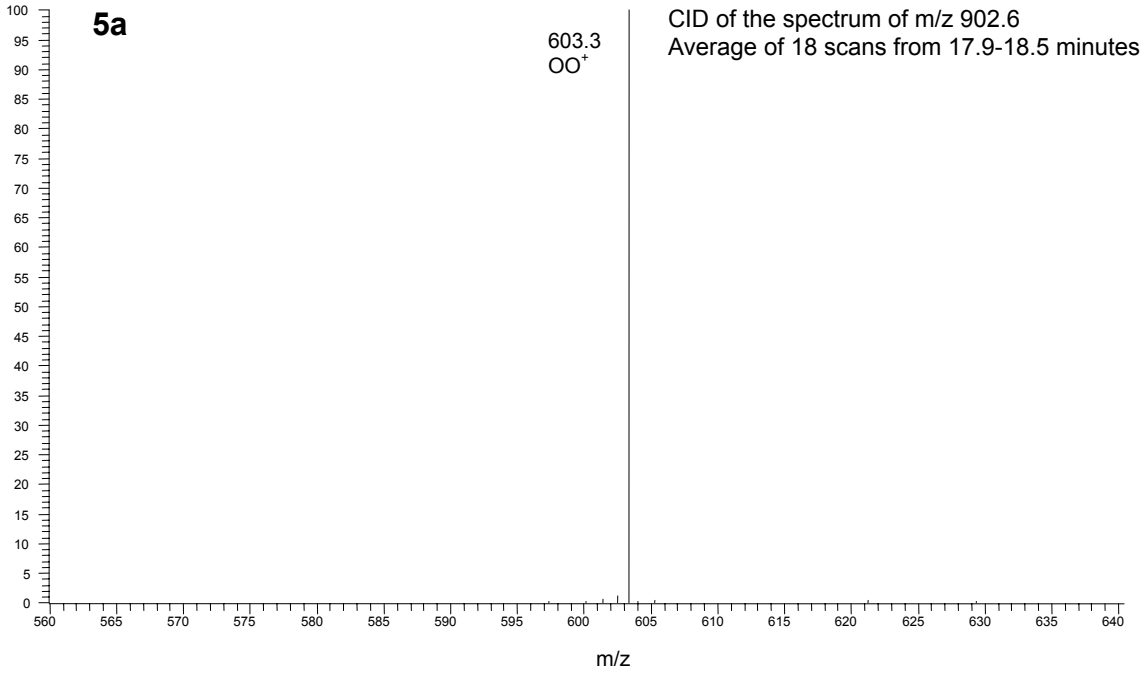
5a
603.3
OO+
CID of the spectrum of m/z 902.6
Average of 18 scans from 17.9-18.5 minutes
m/z

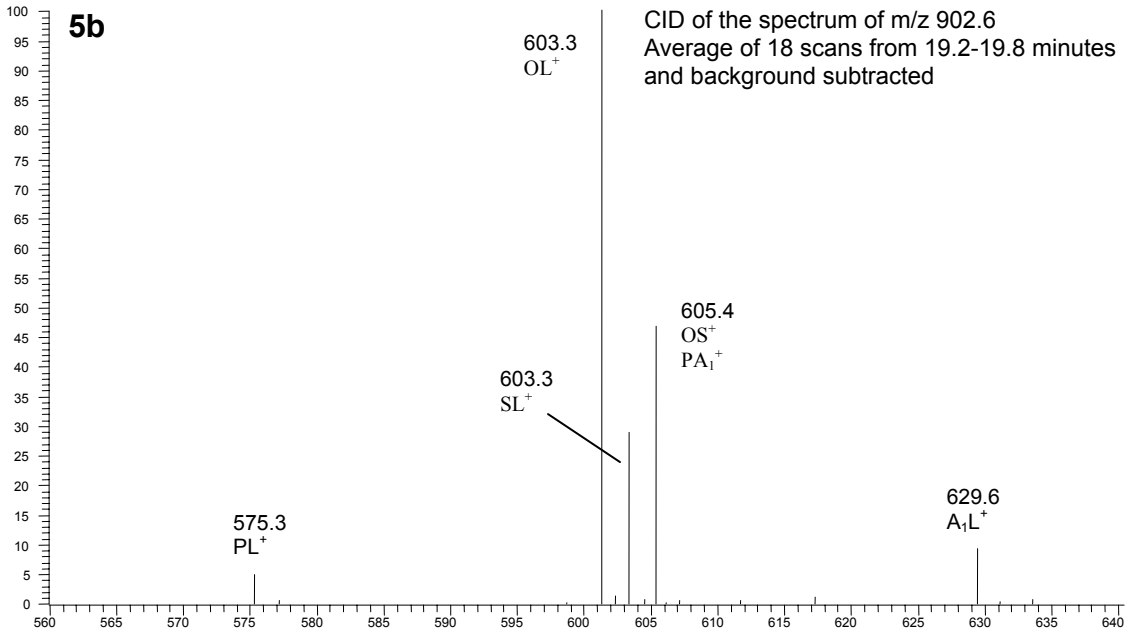
5b
603.3
OL+
CID of the spectrum of m/z 902.6
Average of 18 scans from 19.2-19.8 minutes
and background subtracted
605.4
OS+
PA1+
603.3
SL+
629.6
A1L+
575.3
PL+

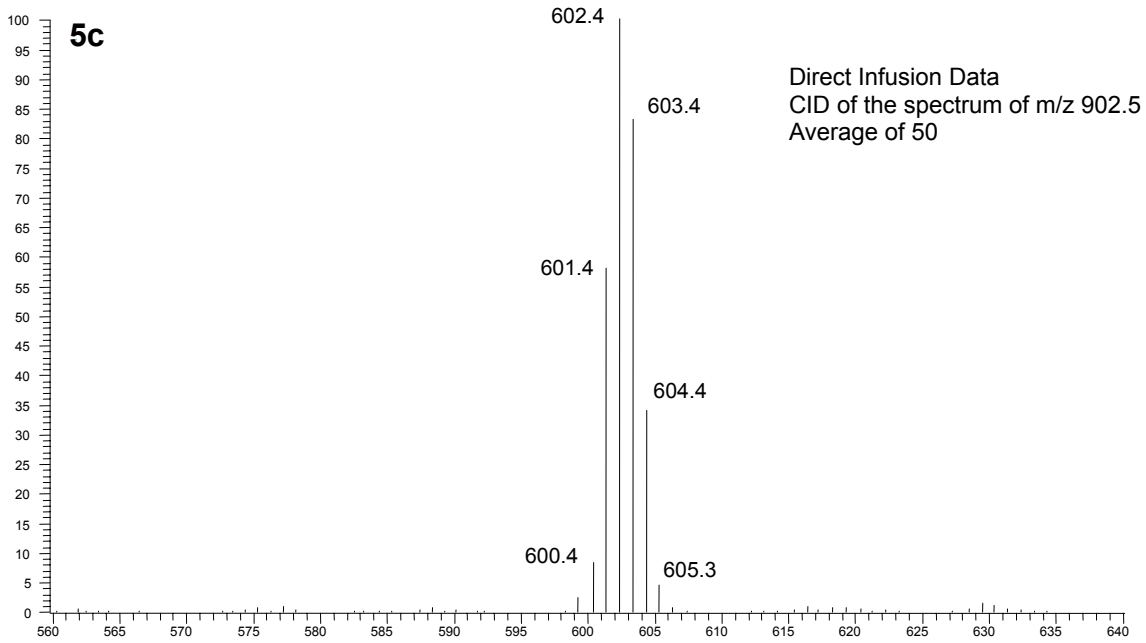

Figure 5. Spectra show the de-convoluted CID spectra of the first (5a) and second (5b) fractions shown in Figure 3a. Through subtraction a representative spectrum of the LOS/LSO/SLO system is obtained that could be used for the quantification of this system of positional isomers. Figure 5c shows the CID spectra of the 902.6 ion acquired via direct infusion-ESI-MS-MS

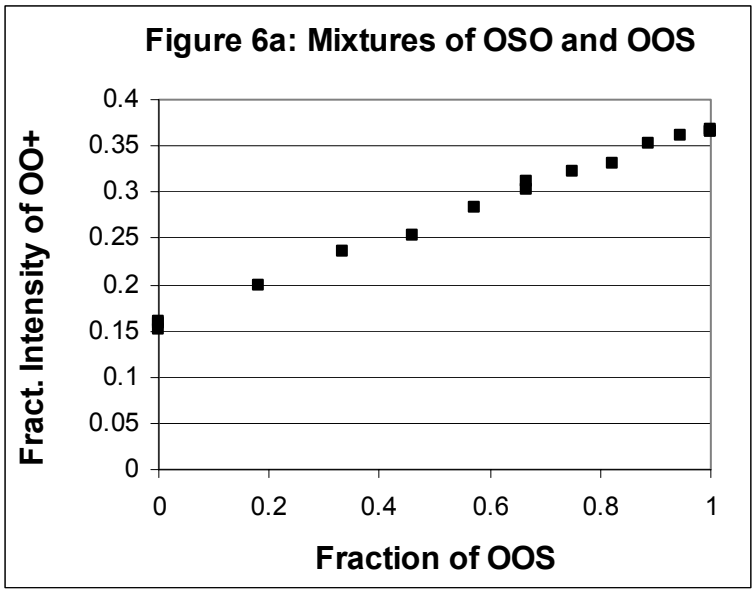
Figure 6a: Mixtures of OSO and OOS
Fract. Intensity of OO+
0.4
0.35
0.3
0.25
0.2
0.15
0.1
0.05
0
0
0.2
0.4
0.6
0.8
1
Fraction of OOS

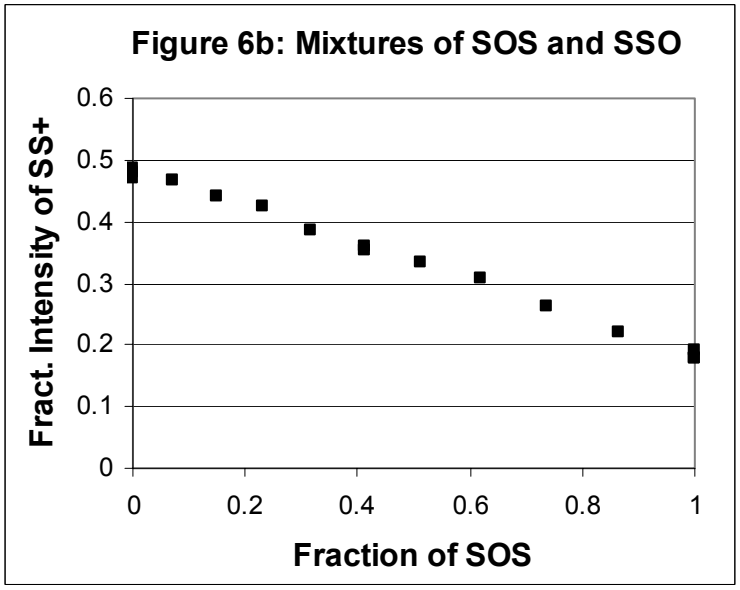
Figure 6b: Mixtures of SOS and SSO
Fract. Intensity of SS+
0.6
0.5
0.4
0.3
0.2
0.1
0
0
0.2
0.4
0.6
0.8
1
Fraction of SOS

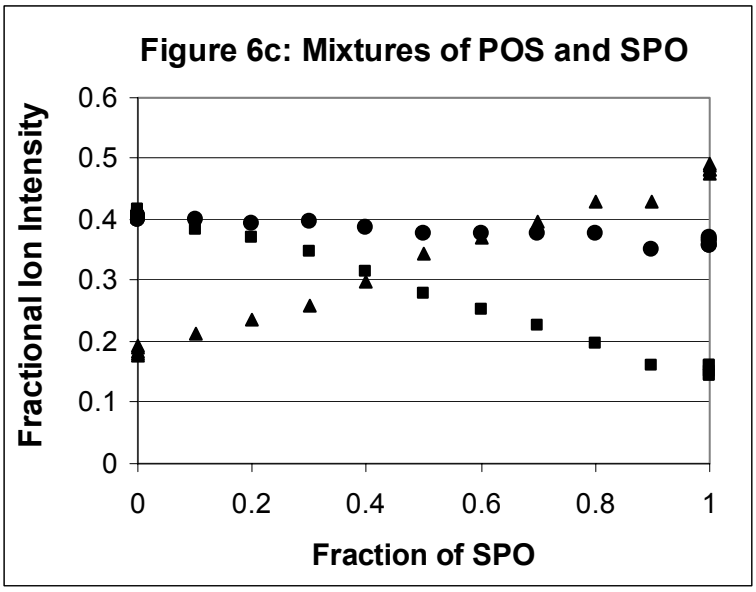
Figure 6c: Mixtures of POS and SPO
Fractional Ion Intensity
0.6
0.5
0.4
0.3
0.2
0.1
0
0
0.2
0.4
0.6
0.8
1
Fraction of SPO

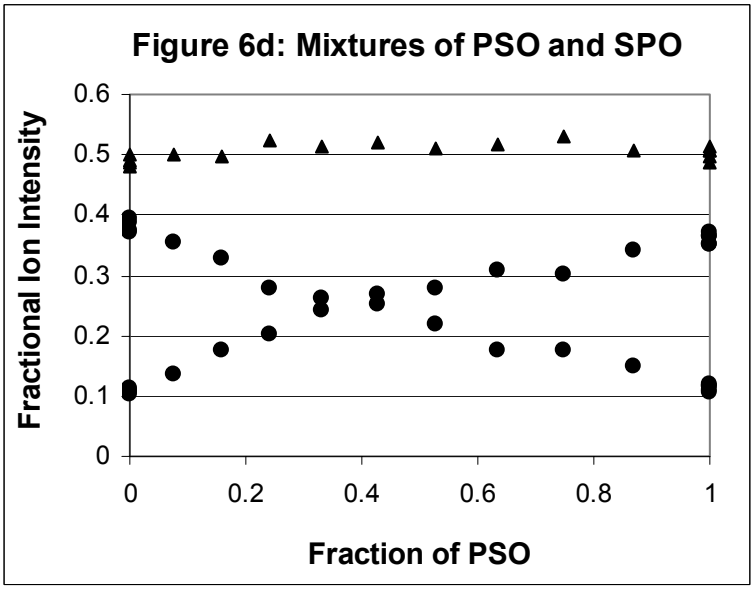
Figure 6d: Mixtures of PSO and SPO
Fractional Ion Intensity
0.6
0.5
0.4
0.3
0.2
0.1
0
0
0.2
0.4
0.6
0.8
1
Fraction of PSO

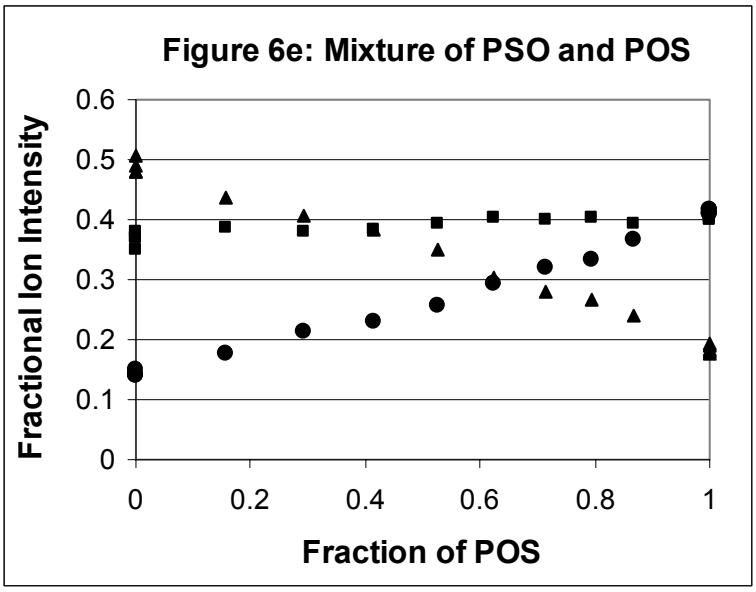

Figure 6a-6e. Calibration plots for binary mixtures of positional isomers. All fractional intensities are relative to the sum of all diglycerol fragments. Figure 6a -Fractional intensities of the SO^+ ion as a function of fractional composition of binary mixtures of OOS and OSO. Fig. 6b -Fractional intensities of the SO^+ ion as a function of fractional composition of binary mixtures of SSO and SOS. Fig. 6c- Fractional intensities of the diglycerol fragments as a function of fractional composition of binary mixtures of POS and SPO. Fig. 6d- Fractional intensities of the diglycerol fragments as a function of fractional composition of binary mixtures of PSO and SPO. Fig. 6e- Fractional intensities of the diglycerol fragments as a function of fractional composition of binary mixtures of PSO and POS. In Fig. 6c-6e ■ represents the fractional intensity of SO^+, ▲ represents the fractional intensity of SP^+, and • represents the fractional intensity of PO^+.

Table 1. Relative intensities of the diglycerol CID fragments $[M+NH_4\text{-}FA+NH_3]^+$ for the standard TAGs analyzed in this work. These data support the general rule that cleavage of the fatty acid in the center position is unfavorable. Data for the LnLnLn, LLL, and LLL are not shown here, because the CID spectra for these simple TAGs are trivial. $LnLn^+$, LL^+, and OO^+, respectively, are the only diglycerol fragments present in the spectra.

TAG	Parent Ion	PP^+	PO^+	SP^+	OO^+	SO^+	SS^+/ AP^+	AO^+	TO^+	TT^+
POP	850.8	16.2	100.0	-	-	-	-	-	-	-
PPO	850.8	100.0	92.8	-	-	-	-	-	-	-
SPO	878.6	-	66.5	100.0	-	22.4	-	-	-	-
POS	878.6	-	100.0	40.7	-	99.0	-	-	-	-
PSO	878.6	-	25.4	100.0	-	67.9	-	-	-	-
OOS	904.8	-	-	-	55.0	100.0	-	-	-	-
OSO	904.8	-	-	-	17.0	100.0	-	-	-	-
SSO	906.6	-	-	-	-	90.0	100.0	-	-	-
SOS	906.6	-	-	-	-	100.0	17.1	-	-	-
APO	906.6	-	69.3	-	-	-	100.0	25.0	-	-
AOP	906.6	-	100.0	-	-	-	41.4	89.9	-	-
PAO	906.6	-	32.6	-	-	-	100.0	63.1	-	-
TOT	1075.0	-	-	-	-	-	-	-	100.0	22.3

Table 2. Fractional composition data of the three isomeric systems analyzed for various oils and fats. The first three columns consist of fractional composition data for the POS/PSO/SPO system. The next two columns give fractional composition data for the SOS/SSO system. The final two columns give fractional composition data for the OOS/OSO system. The designation, "Int", indicates that accurate data could not be obtained due to a co-eluting TAG which interfered with quantification.

Oil/Fat	POS	PSO	SPO	SOS	SSO	OOS	OSO
corn	0.99±0.09	-0.02±0.10	0.16±0.09	Int	Int	0.99±0.05	0.01±0.05
vegetable	1.02±0.09	0.00±0.10	0.00±0.10	Int	Int	1.07±0.10	-0.07±0.101
safflower	0.97±0.09	0.03±0.10	0.04±0.09	Int	Int	1.01±0.04	-0.01±0.04
olive	1.05±0.09	-0.06±0.11	0.08±0.09	Int	Int	1.05±0.06	-0.05±0.06
peanut	1.06±0.09	-0.08±0.12	0.00±0.09	Int	Int	0.98±0.08	0.02±0.08
tanning oil	1.01±0.09	0.05±0.12	0.01±0.09	0.96±.04	0.04±0.04	0.95±0.04	0.05±0.04
cocoa	1.04±0.09	0.04±0.12	0.00±0.10	0.94±.04	0.06±0.04	1.02±0.04	-0.02±0.04
Crisco	0.66±0.10	0.33±0.12	0.00±0.08	0.55±.04	0.45±0.04	0.89±0.04	0.11±0.04
chicken	0.62±0.09	0.29±0.12	0.10±0.08	0.56±.06	0.44±0.06	0.76±0.04	0.24±0.04
beef	0.64±0.09	0.13±0.12	0.23±0.07	0.79±.04	0.21±0.06	1.00±0.04	0.00±0.04
pork	0.08±0.15	-0.12±0.15	1.03±0.05	0.1±0.1	0.9±0.1	Int	Int